Our responses to the comments are as follows: Comments are in black, authors' responses are in blue, and changes to the manuscript are in red color text. Figures prepared for reply are named as Figure R-.

Community comment:

Dear Authors, editor, and reviewers,

This manuscript presents insights into the interactions between sea spray aerosols (SSAs) and aromatic acids through a laboratory study. This is an interesting and valuable research. I have some constructive comments on this manuscript.

Specific comments:

Abstract and Introduction:

Line 11, what is the importance of aromatic acids with SSAs in affecting the global radiative balance? In the following section of Introduction (Lines 29-40), the authors had ambiguous presentation in relationship between SSAs, aromatic acids, and global radiative balance.

Author reply:

As an important medium for exchange processes between ocean and the atmosphere, SSA directly affects the radiative balance of the Earth by scattering solar radiation and indirectly affects the global climate as a source of cloud condensation nuclei and ice nuclei (Wilson et al., 2015; Quinn et al., 2017; Rosenfeld et al., 2019; Croft et al., 2021). It is well known that the presence of surfactants affects the production of SSA, which in turn may affect the global radiation balance. This indicates that aromatic acids as a surfactant may also affect the global radiation balance. We have updated the Introduction section.

Lines 35-38:

Previous studies suggest that these organic acids can alter the composition of SSA, subsequently influencing atmospheric processes such as cloud condensation nuclei (CCN) or ice nuclei (IN) activities. SSA may contain organic acids that play a major role in Earth's climate (Moore et al., 2011; Zhu et al., 2019).

Lines 41-54: The authors introduced the current studies in seawater source of aromatic acids in this paragraph, that is, the majority is from esters released and biodegraded by algae and the remain is from anthropogenic emissions. Could aromatic acids be derived from precipitation? What are the major types and their proportions and concentrations of aromatic acids in seawater? It should correspond to aromatic acids the authors used in the experiments (lines 90-98, 2 Experiment Section). More detailed description and possible summary are needed.

Author reply:

A previous study found benzoic acid in snow pit samples (Mochizuki et al., 2016), while the other aromatic acid samples were not studied in precipitation. The types, sources, and concentrations of the target aromatic acids are summarized in Table S4. The following content has been added to the revised manuscript.

Line 41-45:

In various observations, aromatic acids have been detected in both natural and anthropogenic sources (Zhao et al., 2019; Zangrando et al., 2019; Dekiff et al., 2014). Among them, natural sources of aromatic acids produced by algal releases account for most marine aromatic acids, especially benzoic acid, and most of hydroxybenzoic acids (Mostafa et al., 2017; Fotso Fondja Yao et al., 2010b; Castillo et al., 2023; Abdel-Hamid A. Hamdy, 2020).

Line 50-53:

This is consistent with previous researches that phthalic acid is primarily derived from anthropogenic sources (Ren et al., 2023b), whereas hydroxybenzoic acid has both anthropogenic and natural sources (Zhao et al., 2019; Castillo et al., 2023).

Line 89-90:

Further details are provided in Table S1, which lists sources and concentrations of these aromatic acid identified in seawater and atmospheric samples over the ocean.

Table S1. Sources and concentrations of aromatic acids identified in seawater and atmospheric samples over the ocean.

Aromatic acids	**Natural sources**	**Anthropogenic sources**
benzoic acid	● sea algae (Abdel-Hamid A. Hamdy, 2020; Al-Zereini et al., 2010; Fotso Fondja Yao et al., 2010a; Liu et al., 2022b) ● sedimentary organic matter (10–65 μg g^{-1}) (Deshmukh et al., 2016) ● bacteria isolated from sea bass viscera (314 ppb) (Martí-Quijal et al., 2020) ● snow pit samples (2.11 ng g^{-1}) (Mochizuki et al., 2016)	● emerging endocrine disrupting compounds (34–491 ng L^{-1}) (Zhao et al., 2019) ● fuel combustion (Boreddy et al., 2017) ● industrial wastewater, automobile exhaust and tobacco smoke (Cuadros-Orellana et al., 2006)
o-phthalic acid		● plasticizer (16.7–657 ng g^{-1} d.w.) (Ren et al., 2023a; Sanjuan et al., 2023); ● plastic waste burning (8.3–84.9 ng m^{-3}) (Zhu et al., 2022) ● the end product of photochemical oxidation of SOA (15.5 ng m^{-3}) (Ding et al., 2021) ● biomass burning and fossil fuel combustion sources (0.4–7.9 ng m^{-3}) (Shumilina et al., 2023; Yang et al., 2020; Boreddy et al., 2022)

m-phthalic acid		● plasticizer (Ren et al., 2023a) ● the end product of photochemical oxidation of SOA (3.6 ng m^{-3}) (Ding et al., 2021) ● biomass burning and fossil fuel combustion sources (0.01–2.3 ng m^{-3}) (Yang et al., 2020; Boreddy et al., 2022; Kawamur, 2014)
p-phthalic acid		● plasticizer (0.51–6.8 mg kg^{-1}) (Ren et al., 2023a; Di Giacinto et al., 2023; Di Renzo et al., 2021) ● plastic waste burning (10.8–80.7 ng m^{-3}) (Zhu et al., 2022); the end product of photochemical oxidation of SOA (4.3 ng m^{-3}) (Ding et al., 2021) ● biomass burning and fossil fuel combustion sources (0.05–2.5 ng m^{-3}) (Yang et al., 2020; Boreddy et al., 2022; Kawamur, 2014)
o-hydroxybenzoic acid	● sea algae (76.8 mg L^{-1}) (Castillo et al., 2023; Mostafa et al., 2017; Klejdus et al., 2017)	● pharmaceuticals and drugs of abuse (0.4–53.3 ng L^{-1}) (Alygizakis et al., 2016)
m-hydroxybenzoic acid	● sea algae (Al-Zereini et al., 2010; Castillo et al., 2023)	

p-hydroxybenzoic acid	● sea algae (57.7 mg L^{-1}) (Castillo et al., 2023; Klejdus et al., 2017; Tian et al., 2012; Hawas and Abou El-Kassem, 2017) ● sea fungus (Rukachaisirikul et al., 2010; Shao et al., 2007) ● sponge Mycale species (Xuefeng Zhou, 2013); metabolite (Jingchuan Xue, 2015; Liao and Kannan, 2018) ● sediment samples (6.85–437 ng g^{-1} dw) (Liao et al., 2019)	● Pharmaceuticals and personal care products (Lu et al., 2023) ● emerging endocrine disrupting compounds (4.58–49.9 ng L^{-1}) (Zhao et al., 2019; Lu et al., 2021; Alygizakis et al., 2016)
vanillic acid	● sea algae (3–47 ng L^{-1}) (Zangrando et al., 2019; Klejdus et al., 2017) ● lignin decomposition (Wang et al., 2015; Hu et al., 2022; Xu et al., 2017)	● combustion of both softwood and hardwood (Simoneit, 2022)
syringic acid	● sea algae (0.3–0.6 ng L^{-1}) (Poznyakovsky et al., 2021; Zangrando et al., 2019; Klejdus et al., 2017) ● lignin decomposition (Hu et al., 2022; Xu et al., 2017)	● pharmaceuticals (Fisch et al., 2017) ● hardwood burning (Simoneit, 2022)

Line 80 Sintered glass filter and wave breaking method can also produce artificial SSAs with different properties of flux, chemical composition, size distribution, and so on. The authors should clarify the relationship between methods (sintered glass filter, plunging jet, and wave breaking) and possible efficiency of aromatic acid transport within SSAs. That is, whether the plunging jet method can effectively reflect the “Role of sea spray aerosol at the air-sea interface in transporting aromatic acids to the atmosphere”?

Author reply:

Combining the following parameters, we obtained a particle size distribution similar to that from field observations (Quinn et al., 2017; Xu et al., 2022), which is shown in Fig. S2. The experimental principle aligns with previous successful studies (Sha et al., 2021; Johansson et al., 2019). This enables us to consider that the plunging jet method can effectively reflect the transfer of aromatic acid at the air-sea interface.

The reasons for the selection of the relevant parameters are as follows:

1) A stainless steel nozzle with an inner diameter of 4.3 mm is used to generate plunging jets. The nozzle can be changed easily. The size of the nozzle is consistent with that in previous studies (Salter et al., 2014; Sha et al., 2021).

2) We have studied the cases with headspace heights of 14 cm, 19 cm, and 22 cm in our previous work (Liu et al., 2022a) and found that the SSA production was most efficient at a headspace height of 22 cm. Hence, we chose it for SSA generation.

3) We have tried pump flow rates of 0.50 L min^{-1}, 0.75 L min^{-1}, 1.00 L min^{-1}, 1.25 L min^{-1}, and 1.50 L min^{-1} in our previous study (Liu et al., 2022a) and found that when the pump flow rate was 1 L min^{-1} or higher, the performance of the SSA generator was good (see Table R1). Therefore, we used a pump flow rate of 1 L min^{-1} to maintain a high SSA production rate and a relatively long working lifetime of the corresponding accessories.

Table R1. Effect of pump flow rate on SSA production.

Pump flow rate (L min^{-1})	SSA production (particles s^{-1})	Mass concentration (μg m^{-3})
0.50	5.78×10^6	198.96
0.75	9.90×10^6	317.31
1.00	1.37×10^7	417.86
1.25	1.58×10^7	469.59
1.50	1.63×10^7	495.42

4) We have previously studied SSA production at purge air flow rates of 2 L min^{-1}, 3 L min^{-1}, 4 L min^{-1}, 5 L min^{-1}, 6 L min^{-1} to simulate the sea breeze (Liu et al., 2022a). We found that the SSA production increased with the purge air flow rate when the flow rate was less than 3 L min^{-1}, and decreased with the increase of the purge air when the flow rate was more than 3 L min^{-1}.

5) Based on a previous study of the effect of relative humidity on the growth of sea salt particles, the inlet humidity would affect the morphology of SSA. (Tang et al., 1997). Hence, we chose to keep the relative humidity at about 40% in our study. Particles will deliquescence at higher humidity (Bryan et al., 2022). In addition, it has been demonstrated that acid has no effect on NaCl deliquescence (Ming and Russell, 2001).

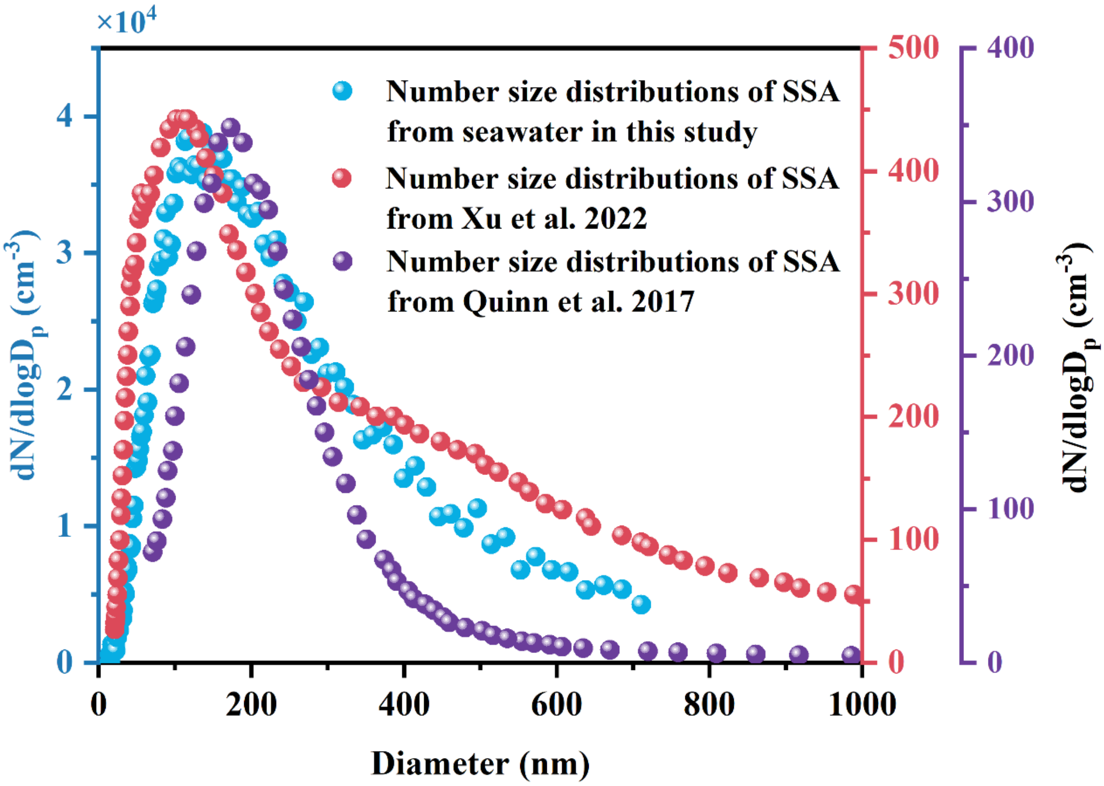

Fig. S2. Number size distribution of SSA generated with the SSA simulation chamber in this study compared with field studies.

Experimental Section

Lines 90-97 Why do authors chose these types of aromatic acids? It should be clarified.

Author reply:

1) Molecular Structure:

Different aromatic acids have distinct properties, including molecular structure, polarity, and reactivity. We aimed to investigate the position and number of functional groups and the effect of different functional groups on the transport of aromatic acids in SSA at the air-sea interface.

2) Biological Significance:

Most aromatic acids we selected are emerging endocrine-disrupting compounds with the potential for bioaccumulation in living organisms (Zhao et al., 2019). The associated human health risks should be of great concern.

3) Climate-Relevant Properties:

Aromatic acids may change the SSA acidity that make them particularly relevant to climate processes (Angle et al., 2021).

In summary, the selection of specific aromatic acids is likely driven by a combination of their molecular structure, biological significance, relevance to climate processes, and practical considerations for experimentation or observation.

Lines 93-94 The collection procedure of seawater is not clear (site, chemical composition of seawater, contamination control, storge conditions, filtration or not?) Detailed QA/QC description is needed.

Author reply:

We have indicated the collection procedure of seawater in the revised Supplement to make the experimental process clearer.

S1. Quality assurance/quality control.

Seawater was collected from the coastal area of Shazikou on March 27, 2023, with a volume of 500 L (Fig. S1). Considering the storage inconvenience caused by huge consumption of seawater, all our seawater was pre-filtered through a polyethersulfone filter (47 mm diameter, 0.2 μm pore size, Supor®-200, Pall Life Sciences, USA) and stored in the dark at 18 °C for less than one month. Quinn et al. (2015) have shown that the fraction that passes through the filter is regarded as dissolved organic carbon and includes colloidal and truly dissolved materials. For each experiment, we measured particle number concentrations generated by filtered seawater and cations concentrations in seawater, and we found good agreement between each set of experiments (see Fig. S2).

In order to avoid the influence of organic matter in quartz fiber filters and access the accuracy of the experiment, pre-baked quartz fiber filters were used in sampling. Before each set of experiments, experimental blanks were conducted using filtered seawater. Experimental blanks were conducted with the same procedure of SSA samples. Seawater and filter samples were stored at -20°C until analyzed. In order to reduce the influence of organic acids residue after each experiment, the SSA simulation chamber was cleaned with ethanol first, then the system was cleaned with ultra-pure water for several times. The above steps also run the pump to allow for thorough cleaning of the system. Therefore, the system was blown with zero air and sealed for preservation. The Dekati DLPI was also ultrasonicated with methanol and water (V:V=1:1) and dried after the experiment.

Filtered seawater (without added aromatic acid) was used as the experimental blank, and the same experimental and analytical methods were used as those for the experimental samples. As a result, no target aromatic acid was found in both seawater and filters. This may be due to the fact that we did not perform any concentration operation during the seawater sample processing. The standard curves for each aromatic acid are linear, as shown in Fig. S5.

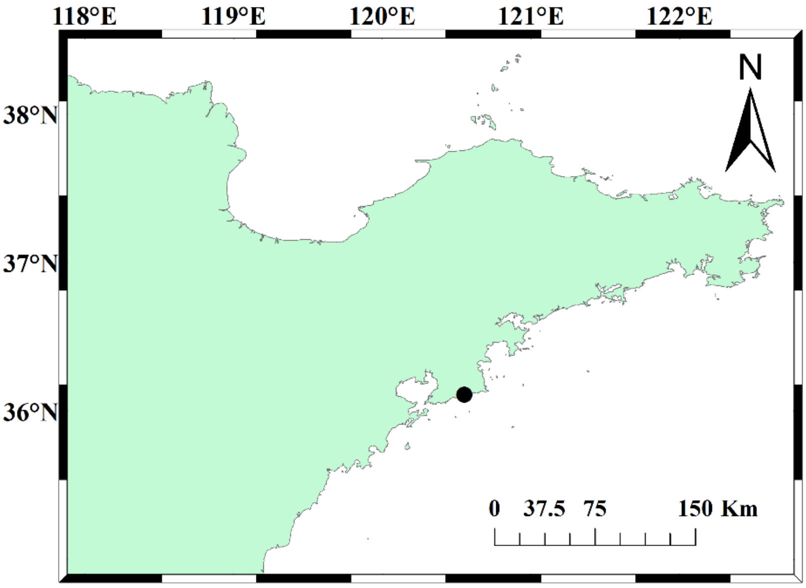

Fig. S1. Sampling site at Shazikou along the Yellow Sea coast, Qingdao, China.

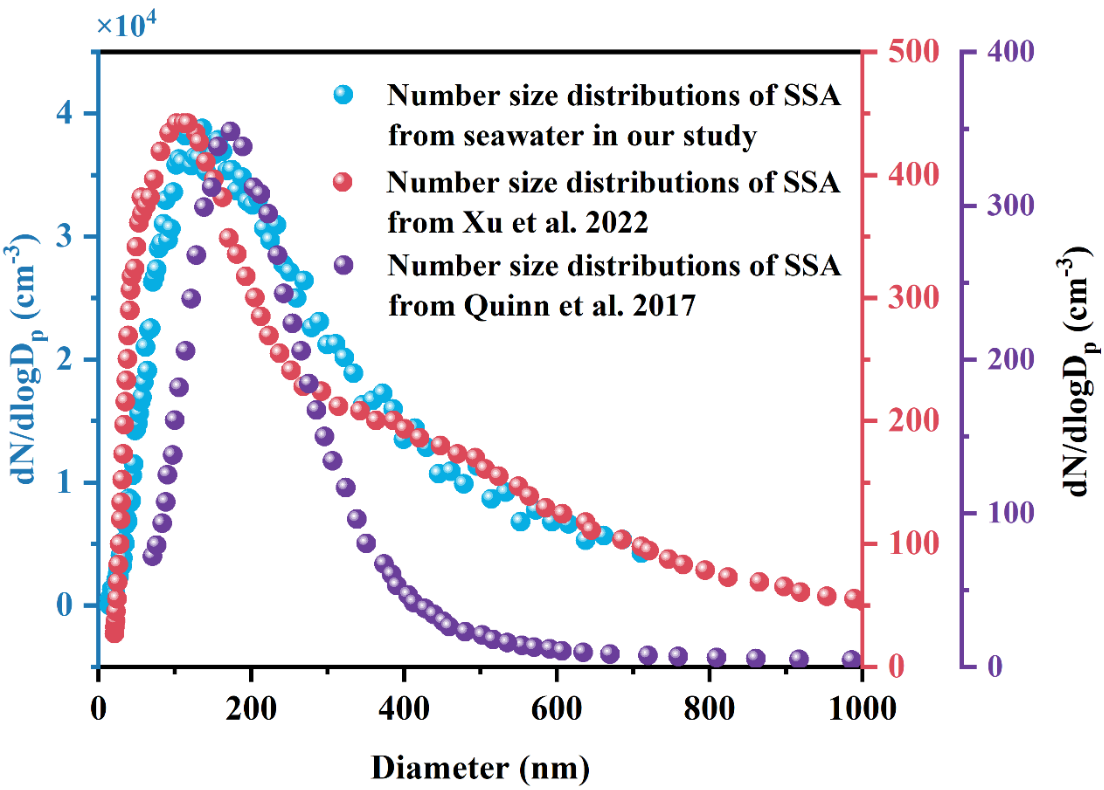

Fig. S2. Number size distribution of SSA generated with the SSA simulation chamber in this study compared with field studies.

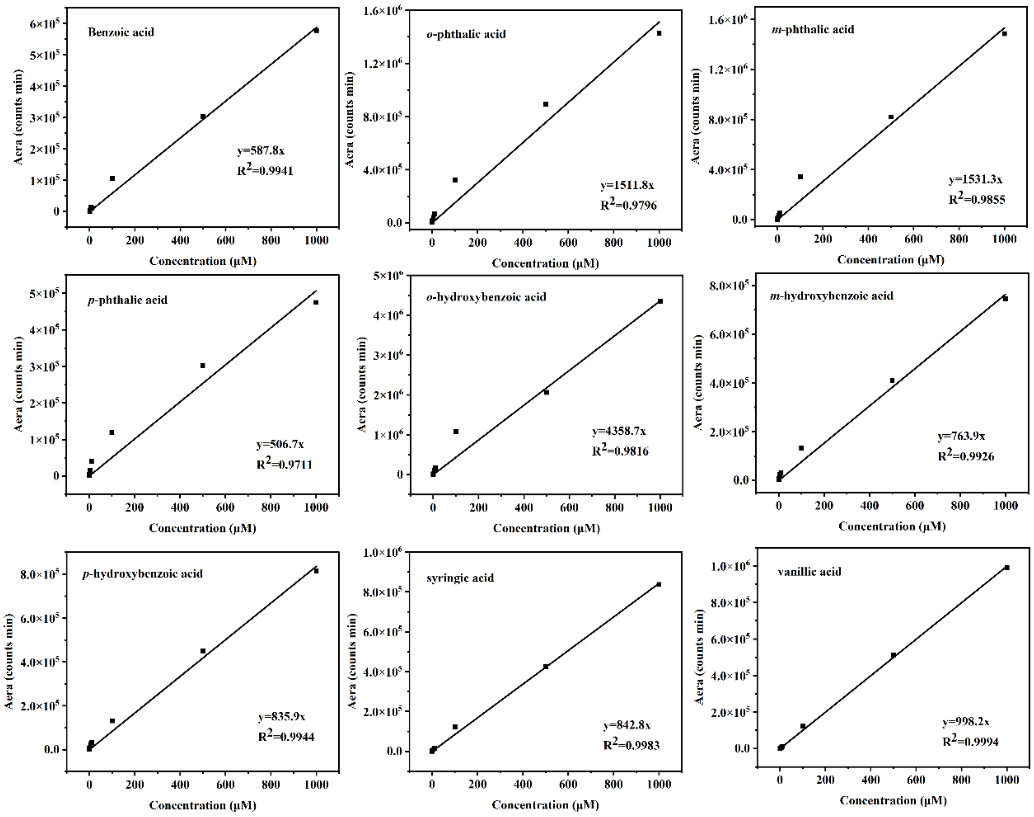

Fig. S5. The standard curves for aromatic acids were constructed within a concentration range of 0.01-1000 μM, with more than seven data points.

Line 98: What is the mass concentration of typical aromatic acids in true seawater, which determines whether the concentration of aromatic acid used in the experiment (1 mM) is reasonable.

Author reply:

The concentration of aromatic acids in seawater ranges from 1 pM to 0.5 mM. To investigate the influence of concentration, we introduced a set of experiments using artificial seawater with a concentration of 1 μM for aromatic acids, and the specific experimental groups can be found in Table S3.

Lines 176-177:

The experiment consisted of a total of 25 sets with target compound concentrations of 10^{-3} and 1 mM (Table S3).

Table S3. Summary of experimental conditions.

Exp. No.	Experiment type	Concentration (mM)	pH	Salinity (psu)	Sampling time (h)	RH (%)	Temperature difference (°C) [a]
1	SW	0	7.92	34.2	5	35	2.0
2	SW+benzoic acid	1	7.72	34.3	5	34	1.5
3	SW+*o*-hydroxybenzoic acid	1	7.60	34.5	5	36	1.0
4	SW+*m*-hydroxybenzoic acid	1	7.68	34.1	5	40	2.0
5	SW+*p*-hydroxybenzoic acid	1	7.84	34.3	5	38	1.5
6	SW+*o*-phthalic acid	1	7.58	34.2	5	36	2.0
7	SW+*m*-phthalic acid	1	7.80	34.5	5	37	2.5
8	SW+*p*-phthalic acid	1	7.85	34.4	5	42	2.0
9	SW+vanillic acid	1	7.81	34.2	5	43	3.0
10	SW+syringic acid	1	7.84	34.3	5	39	2.0
11	ASW	0	7.96	35.1	5	33	1.5
12	ASW+benzoic acid	1	7.68	34.6	5	35	1.0
13	ASW+*o*-hydroxybenzoic acid	1	7.76	34.9	5	34	0.5
14	ASW+*m*-hydroxybenzoic acid	1	7.99	35.3	5	36	1.5
15	ASW+*p*-hydroxybenzoic acid	1	7.85	34.7	5	38	2.0
16	ASW+*o*-phthalic acid	1	7.93	34.5	5	35	1.0

17	ASW+*m*-phthalic acid	1	7.88	34.9	5	36	1.0
18	ASW+*p*-phthalic acid	1	7.97	34.6	5	34	1.5
19	ASW+vanillic acid	1	7.89	35.2	5	35	1.0
20	ASW+syringic acid	1	7.99	34.8	5	39	1.0
21	ASW+benzoic acid+*o*-hydroxybenzoic acid+*o*-phthalic acid+vanillic acid+syringic acid	10^{-3}	7.95	35.1	20	41	3.5
22	ASW+benzoic acid+*m*-hydroxybenzoic acid+*m*-phthalic acid+vanillic acid+syringic acid	10^{-3}	7.98	34.6	20	38	1.5
23	ASW+benzoic acid+*p*-hydroxybenzoic acid+*p*-phthalic acid+vanillic acid+syringic acid	10^{-3}	7.88	34.9	20	40	2.0
24	NaCl	0	7.68	35.3	5	38	1.0
25	NaCl+*m*-hydroxybenzoic acid	1	7.54	34.7	5	36	1.5

[a] The temperature difference in the SSA simulation chamber before and after the experiment.

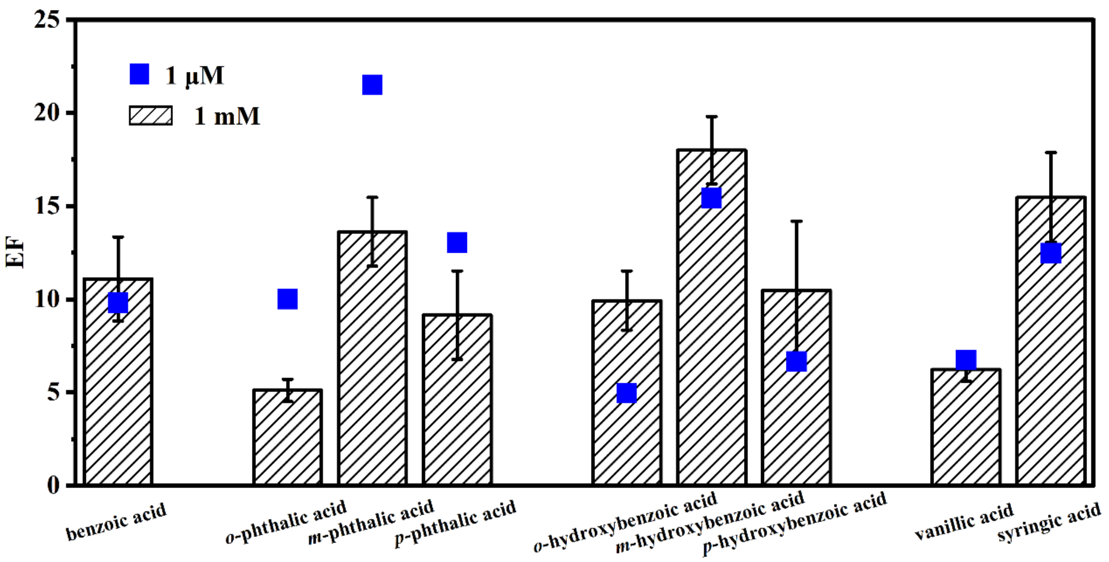

Fig. S8. Enrichment factors of aromatic acids at different concentrations from artificial seawater to the atmosphere.

Comparing the EF of aromatic acids in SW and ASW, it was observed that the EF trends of benzene dicarboxylic acids in seawater follows the pattern: *o*-phthalic acid < *m*-phthalic acid < *p*-phthalic acid. However, in ASW, the EF of *p*-phthalic acid was lower than that of *m*-phthalic acid. Based on the findings of Li et al. (2023), we hypothesize that in ASW, *p*-phthalic acid acts as an ·OH scavenger to produce TAOH. Hence, the EF of *p*-phthalic acid is lower than that of *m*-phthalic acid. Meanwhile, organic compounds in SW preferentially react with ·OH (Anastasio and Newberg, 2007), thus the EF of *p*-phthalic acid is the highest among the benzene dicarboxylic acids. Furthermore, differences in aromatic acid concentration did not change the enrichment pattern of organic acids.

Line 135 Can this flow rate of 1 mL min^{-1} for 1 h collect particles? If so, possible sampling artifacts should be considered. I think this flow rate is too small and cannot achieve/tune with DKL-2.

Author reply:

This has been corrected. The sampling flow rate of the single particle sampler was set to 1 L min^{-1}, which was previously written incorrectly.

Lines 141-142:

The SSA particles impacted onto copper grids films (T11023, Tianld, China) with a flow rate 1 L min^{-1} for 1 h.

Results and discussion

Section 3.2.2 and Fig. 4

How quantitatively determine the thickness of organic coating of collected individual particles and what is the basis of the order? Can thickness of organic coating of selected individual particles represent the whole populations? Is there a statistic bias using only one typical TEM image?

Author reply:

We measured the thickness of most of the organic coating in the field of view, and the ordering was based only on the position of the functional groups of the aromatic acids, not on the thickness. We have modified corresponding figures in the revised manuscript.

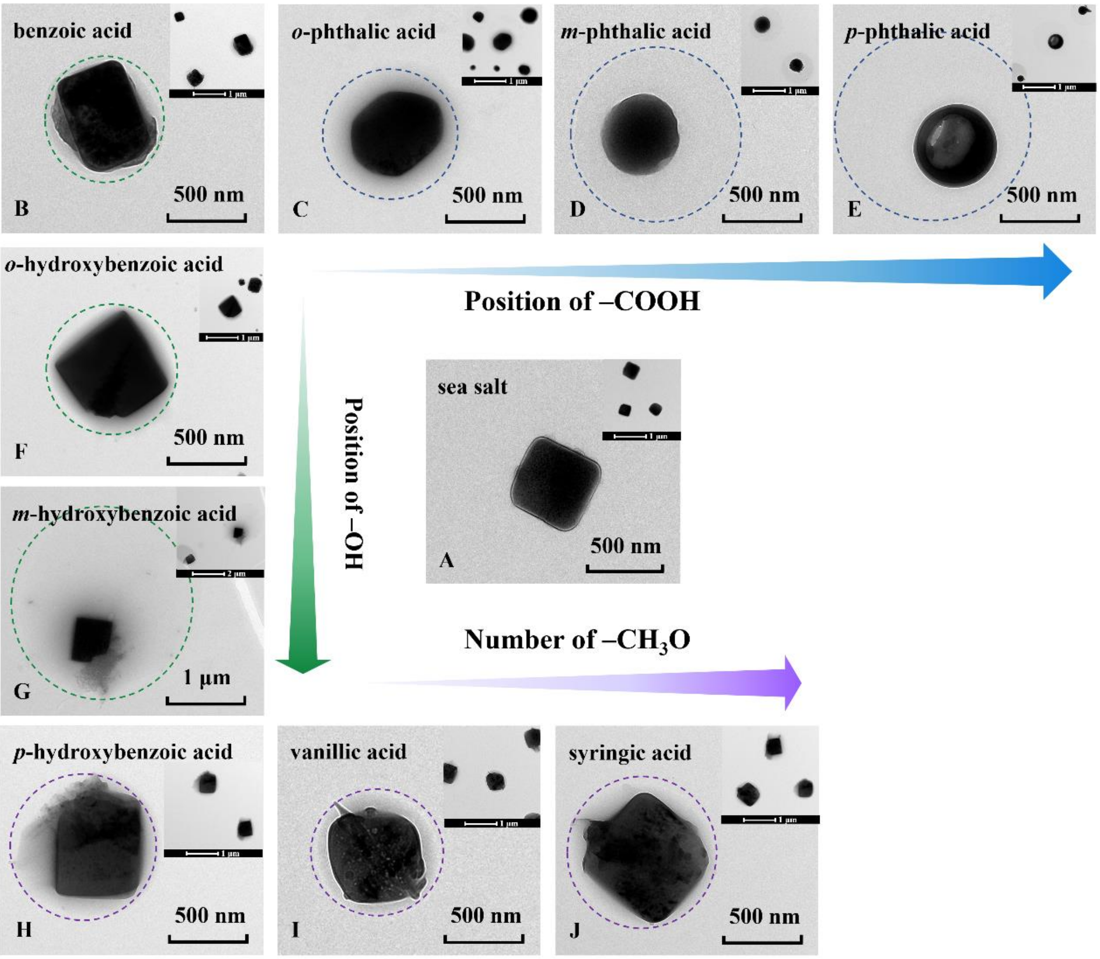

Fig. 4. Particle morphology observed using TEM of sea salt (A) and mixed particles composed of aromatic acids-coated sea salt particles (B–K).

Section 3.3

How many samples were used to calculate the enrichment factors of aromatic acids and cations (both in Figures 5 and 6)? It should be summarized as a new table. The authors performed size-resolved filter-based experiments, what is the level of enrichment factors of aromatic acids in different size?

Author reply:

1) At least three filter samples should be used to calculate the enrichment factor of aromatic acids and cations. We have provided a summary in a new table.

2) In SSA, the ratios of inorganic salts and organic compounds vary with the particle size, which provides an insight into the size resolved enrichment of particulate mass (Bertram et al., 2018; Quinn et al., 2014). Sea salts account for a large fraction of super-micron aerosol particles. With the decrease of particle size, not only does the concentration of organic matter in submicron aerosol particles become higher, but the atmospheric residence time becomes longer (Ault et al., 2013; O'Dowd et al., 2004; Triesch et al., 2021). The global emission of submicron SSA is about 24 Tg y^{-1}, of which organic matter accounts for 8.2 Tg y^{-1} (Meskhidze et al., 2011; Vignati et al., 2010). Although the understanding of organic compounds in submicron SSA has improved considerably in recent years, the transport process of organic acids as typical organic compounds in seawater remains poorly investigated. Then, we just collected all submicron SSA to calculate the enrichment factor.

Table R3. Enrichment factors for aromatic acids in submicron SSA.

Aromatic acid	EF_1	EF_2	EF_3	EF_4	Average EF	Standard deviation
benzoic acid	8.14	17.59	4.34	8.19	9.57	4.89
o-hydroxybenzoic acid	5.13	6.55	8.55		6.74	1.72
m-hydroxybenzoic acid	29.72	29.13	15.21		24.69	8.21
p-hydroxybenzoic acid	10.87	14.81	9.22	13.71	12.15	2.56
o-phthalic acid	4.89	6.14	6.89		5.97	0.83
m-phthalic acid	7.80	6.70	5.68		6.73	0.86
p-phthalic acid	11.53	15.28	12.75	16.80	14.09	2.39
vanillic acid	6.69	8.87	24.22		13.26	2.55
syringic acid	23.50	34.38	15.51		24.46	4.47

The authors hypothesize that the binding effect of Ca^{2+} with aromatic acid is a reason for observed positive enrichment of aromatic acids. In fact, the positive calcium enrichment is also observed using artificial seawater without organic matters (Salter et al., 2016). Therefore, this hypothesis may need additional control experiments, for example, using pure NaCl solution with addition of aromatic acids, to excluded the effect of Ca^{2+}.

Author reply:

We supplemented two sets of control experiments by adding *m*-hydroxybenzoic acid to ASW and NaCl solution to exclude the effect of Ca^{2+}.

Lines 345-347:

Taking *m*-hydroxybenzoic acid as an example, we calculated the enrichment factors of Ca^{2+} and *m*-hydroxybenzoic acid in NaCl solution, ASW and SW, and found that both follow the pattern: $EF_{NaCl} < EF_{ASW} < EF_{SW}$.

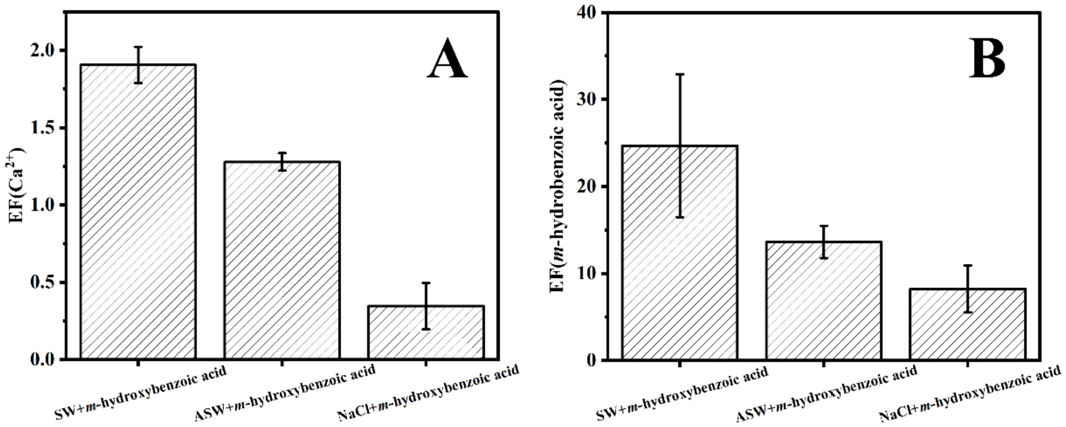

Fig. S9. Enrichment factors of Ca^{2+} and *m*-hydroxybenzoic acid in submicron SSA with SW, ASW, and NaCl solution.

Lines 313-326 I found a missing detail in authors evaluate the cation enrichments, that is, the detailed mass concentration ratio of cations to Na^{+}, for example of Ca^{2+}/Na^{+}, in both seawater and aerosol samples is missing. I therefore suggest the authors supplement more details in mass concentration ratio of aromatic acids and cations in seawater and aerosol samples as a new table.

Author reply:

We give the values of enrichment factors for cations and aromatic acids, as well as their peak areas. Since the standard curves are all linear, we directly used the peak area ratios to derive the enrichment factor values. We have also supplemented the standard curve as follows.

Table R4. Enrichment factors for cations in submicron SSA.

Aromatic acid	Cation	EF_1	EF_2	EF_3	EF_4
benzoic acid	K	0.56	0.57	0.56	0.54
	Mg	0.99	0.84	0.87	1.05
	Ca	1.33	1.27	1.08	1.04
o-phthalic acid	K	0.67	0.91	0.94	
	Mg	1.34	0.73	0.57	
	Ca	0.96	1.26	1.13	
m-phthalic acid	K	0.87	0.82	0.85	
	Mg	0.81	0.76	0.78	
	Ca	1.20	1.32	1.29	
p-phthalic acid	K	0.55	0.77	1.10	0.88
	Mg	0.68	0.73	0.93	0.86
	Ca	1.74	1.18	1.17	1.49
o-hydroxybenzoic acid	K	0.52	0.40	0.88	
	Mg	0.77	1.05	0.98	
	Ca	0.83	1.01	1.71	
m-hydroxybenzoic acid	K	0.90	0.71	1.03	
	Mg	0.77	0.75	0.78	
	Ca	1.97	1.74	2.00	
p-hydroxybenzoic acid	K	0.65	0.67	0.72	0.76
	Mg	0.88	0.81	0.74	0.76
	Ca	1.10	1.00	0.84	1.16
vanillic acid	K	0.91	0.63	0.77	
	Mg	0.79	0.78	1.01	
	Ca	1.95	1.64	0.94	
syringic acid	K	0.95	0.99	0.74	
	Mg	0.92	0.94	0.99	
	Ca	1.79	1.55	1.83	

Table R5. Peak areas of cations in seawater and SSA filter samples.

		SW/10000	SSA/10	SW/10000	SSA/10	SW/10000	SSA/10	SW/10000	SSA/10
benzoic acid	Na	2.11	4.43	2.01	3.01	2.42	4.64	2.41	4.40
	K	0.09	0.11	0.17	0.15	0.09	0.10	0.09	0.09
	Mg	0.54	1.12	0.57	0.72	0.60	1.00	0.51	0.98
	Ca	0.31	0.86	0.39	0.73	0.32	0.67	0.30	0.57
o-phthalic acid	Na	2.39	4.85	2.57	4.46	2.40	4.21		
	K	0.09	0.12	0.08	0.13	0.09	0.15		
	Mg	0.55	1.49	0.52	0.66	0.56	0.56		
	Ca	0.31	0.60	0.33	0.72	0.36	0.71		
m-phthalic acid	Na	2.47	4.49	2.55	4.51	2.52	4.40		
	K	0.10	0.16	0.10	0.14	0.10	0.15		
	Mg	0.60	0.87	0.63	0.85	0.57	0.78		
	Ca	0.33	0.73	0.31	0.72	0.38	0.87		
p-phthalic acid	Na	2.53	5.13	2.67	7.57	2.43	6.67	2.57	6.52
	K	0.12	0.13	0.17	0.38	0.10	0.30	0.09	0.20
	Mg	0.60	0.82	0.63	1.30	0.59	1.50	0.60	1.32
	Ca	0.48	1.70	0.48	1.59	0.40	1.28	0.40	1.52
o-hydroxybenzoic acid	Na	2.96	5.57	2.70	6.80	2.72	6.90		

	K	0.09	0.09	0.11	0.11	0.11	0.25		
	Mg	0.56	0.81	0.63	1.68	0.62	1.54		
	Ca	0.30	0.47	0.32	0.82	0.29	1.24		
m-hydroxybenzoic acid	Na	2.58	4.34	2.55	3.87	2.67	4.37		
	K	0.10	0.15	0.10	0.11	0.10	0.17		
	Mg	0.59	0.76	0.65	0.74	0.60	0.76		
	Ca	0.38	1.27	0.36	0.94	0.36	1.19		
p-hydroxybenzoic acid	Na	2.45	4.82	2.54	4.99	2.63	4.99	2.49	4.59
	K	0.09	0.12	0.10	0.13	0.09	0.12	0.10	0.14
	Mg	0.61	1.06	0.61	0.97	0.62	0.86	0.60	0.84
	Ca	0.48	1.03	0.49	0.96	0.46	0.74	0.41	0.88
vanillic acid	Na	2.53	5.23	2.75	5.06	2.68	5.06		
	K	0.10	0.19	0.12	0.14	0.14	0.20		
	Mg	0.56	0.92	0.69	0.99	0.59	1.13		
	Ca	0.25	1.01	0.50	1.50	0.40	0.71		
syringic acid	Na	2.39	4.98	2.81	5.14	2.99	4.70		
	K	0.09	0.17	0.08	0.15	0.09	0.10		
	Mg	0.51	0.99	0.41	0.71	0.58	0.91		
	Ca	0.28	1.04	0.25	0.70	0.37	1.06		

Table R2. Peak areas of aromatic acids in seawater and SSA filter samples.

	SW$_1$	SSA$_1$	SW$_2$	SSA$_2$	SW$_3$	SSA$_3$	SW$_4$	SSA$_4$
benzoic acid	159632	2732.77	196860	5206.99	185135	1540.1	167892	2508.47
o-phthalic acid	123785	1226.6	168974	1802.2	156324	1888.7		
m-phthalic acid	466987	6606.85	458769	5432.25	491623	4880.15		
p-phthalic acid	454593	10626.92	496102	21471.43	445985	15614.82	471582	20110.87
o-hydroxybenzoic acid	257548	2482	232946	3844.08	238358	5167.06		
m-hydroxybenzoic acid	170482	8532.59	160309	7072.09	190181	4732.93		
p-hydroxybenzoic acid	169753	3635.99	153257	4467.54	131186	2297.87	171062	4329.58
vanillic acid	357000	4948.01	287470	4696.83	279462	12750.11		
syringic acid	486640	23833.92	467129	29328.75	491816	11993.31		

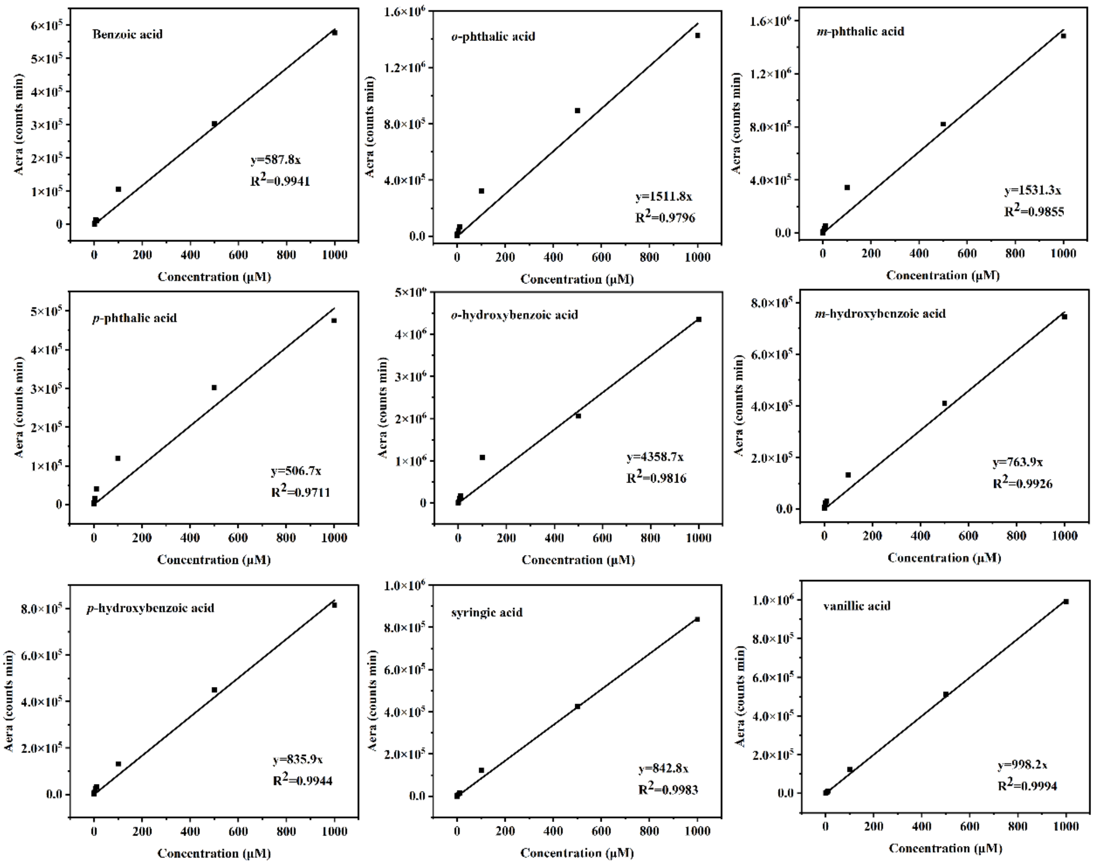

Fig. S5. The standard curves for aromatic acids were constructed within a concentration range of 0.01-1000 μM, with more than seven data points.

Minor comments:

Lines 57: Please clarify “a potential route”.

Author reply:

In our response to other previous Reviewers’ comments, we have updated the related sentence.

Lines 57-59:

One possible reason for the disappearance of these aromatic acids is their release into the atmosphere. Existing datasets obtained from remote marine areas offer evidence of the presence of these compounds in the atmosphere (Fu et al., 2010).

Lines 59-62: This sentence is hard to follow. What is that sea-salt included organic surfactants can thereby further disturbing ecological systems? The cited references also seem inappropriate.

Author reply:

We have rewritten this sentence.

Lines 61-63:

SSAs can act as carrier agents for the vertical transport of much more than just sea salt and often include organic surfactants in the ocean, as already shown by field and laboratory studies (Cochran et al., 2016; Franklin et al., 2022; Rastelli et al., 2017).

Line 109 What is the air flow rate? It should be different in different experiment procedures.

Author reply:

We have updated Fig. S2 to provide a clearer figure of the air flow rate during the experiment.

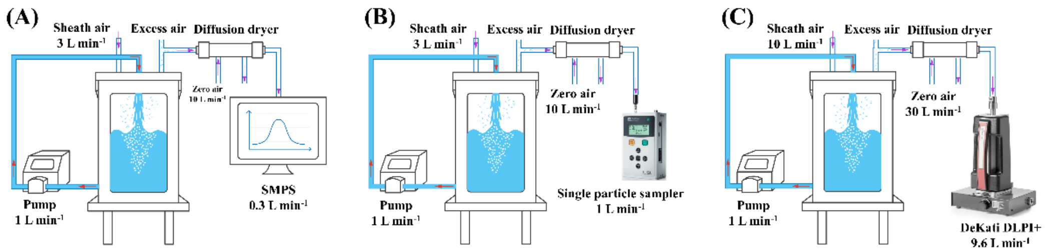

Fig. S2. Schematic picture of the plunging jet-sea spray aerosol generator: SMPS sampling (A), single particle sampling (B), and DeKati DLPI+ sampling (C). The red arrows represent the flow direction of seawater, and the purple arrows represent the flow of gases and aerosol particles.

Fig.3 It is hard to follow the differences in particle size, because these circles are almost identical.

Author reply:

We have labelled the particle sizes in Figure 3.

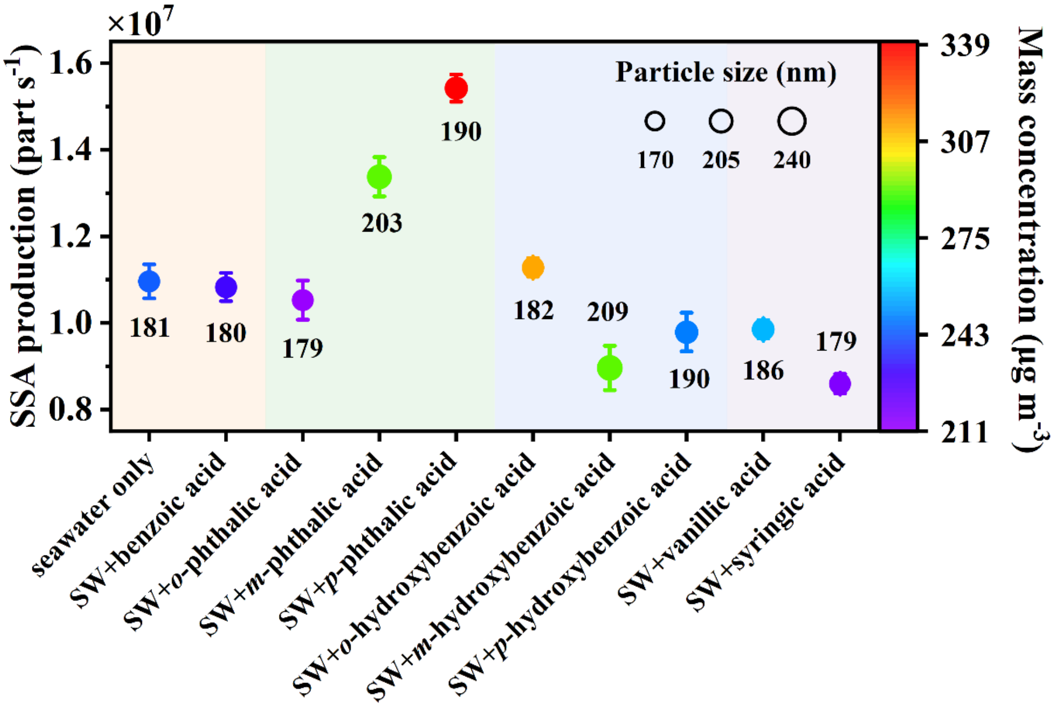

Fig. 3. SSA production, particle size, mass concentration distribution of aromatic acids. The symbol size represents the geometric mean diameter of SSA particles and is marked with numbers, and the symbol color indicates the particle mass concentration.

Fig.4 It is hard to follow the colors of subplots A, B, and C. The color span between groups should be larger.

Author reply:

We have updated the figure to expand the color span between the groups.

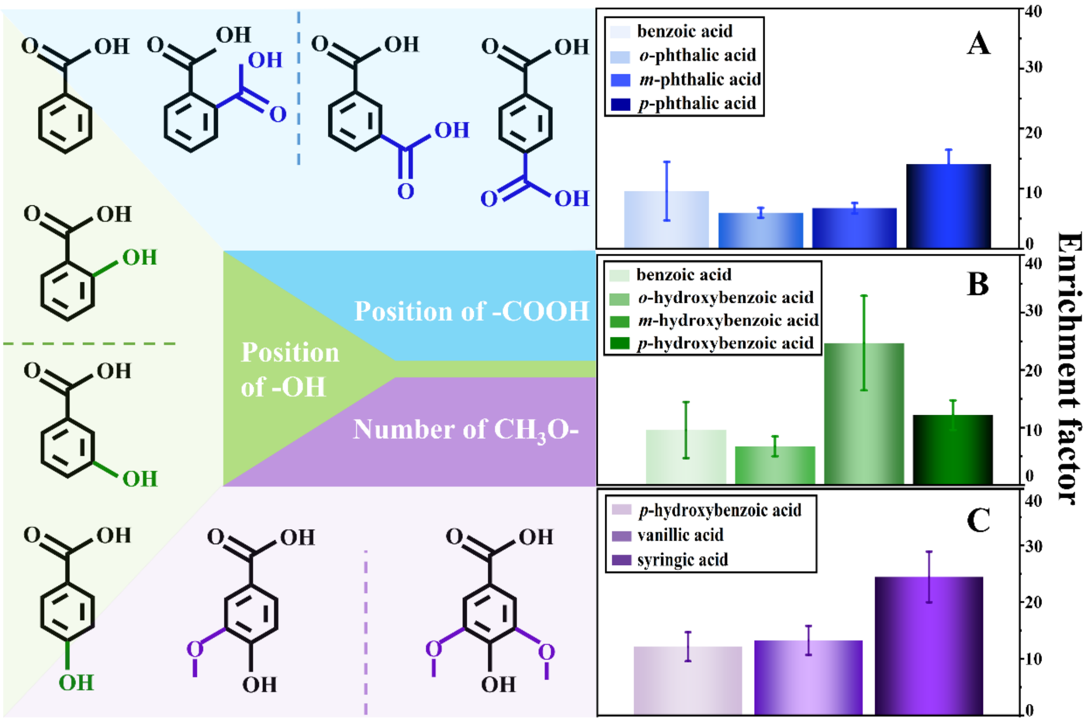

Fig. 5. Enrichment factors of benzene dicarboxylic acids (A), hydroxybenzoic acids (B), *p*-hydroxybenzoic acid, vanillic acid, and syringic acid (C) from seawater to the atmosphere.

Reference

Salter, M. E., Hamacher-Barth, E., Leck, C., Werner, J., Johnson, C. M., Riipinen, I., Nilsson, E. D., and Zieger, P.: Calcium enrichment in sea spray aerosol particles, Geophys Res Lett, 43, 8277-8285, https://doi.org/10.1002/2016gl070275, 2016.

References

Abdel-Hamid A. Hamdy, N. M. E.-f., A. El-Beih, M. Mohammed, W. Mettwally: Egyptian red sea seagrass as a source of biologically active secondary metabolites, Egyptian Pharmaceutical Journal 19, 224, 10.4103/epj.epj_57_19, 2020.

Al-Zereini, W., Fotso Fondja Yao, C. B., Laatsch, H., and Anke, H.: Aqabamycins A-G: novel nitro maleimides from a marine Vibrio species. I. Taxonomy, fermentation, isolation and biological activities, J. Antibiot., 63, 297–301, 10.1038/ja.2010.34, 2010.

Alygizakis, N. A., Gago-Ferrero, P., Borova, V. L., Pavlidou, A., Hatzianestis, I., and Thomaidis, N. S.: Occurrence and spatial distribution of 158 pharmaceuticals, drugs of abuse and related metabolites in offshore seawater, Sci. Total Environ., 541, 1097–1105, 10.1016/j.scitotenv.2015.09.145, 2016.

Anastasio, C. and Newberg, J. T.: Sources and sinks of hydroxyl radical in sea-salt particles, J. Geophys. Res. Atmos., 112, D10306, 10.1029/2006jd008061, 2007.

Angle, K. J., Crocker, D. R., Simpson, R. M. C., Mayer, K. J., Garofalo, L. A., Moore, A. N., Mora Garcia, S. L., Or, V. W., Srinivasan, S., Farhan, M., Sauer, J. S., Lee, C., Pothier, M. A., Farmer, D. K., Martz, T. R., Bertram, T. H., Cappa, C. D., Prather, K. A., and Grassian, V. H.: Acidity across the interface from the ocean surface to sea spray aerosol, Proc. Natl. Acad. Sci. U.S.A., 118, e2018397118, 10.1073/pnas.2018397118, 2021.

Boreddy, S. K. R., Hegde, P., Arun, B. S., Aswini, A. R., and Babu, S. S.: Molecular composition and light-absorbing properties of organic aerosols from west-coast of tropical India, Sci. Total Environ., 845, 157163, 10.1016/j.scitotenv.2022.157163, 2022.

Boreddy, S. K. R., Mochizuki, T., Kawamura, K., Bikkina, S., and Sarin, M. M.: Homologous series of low molecular weight (C1-C10) monocarboxylic acids, benzoic acid and hydroxyacids in fine-mode (PM2.5) aerosols over the Bay of Bengal: Influence of heterogeneity in air masses and formation pathways, Atmos. Environ., 167, 170–180, 10.1016/j.atmosenv.2017.08.008, 2017.

Bryan, C. R., Knight, A. W., Katona, R. M., Sanchez, A. C., and Schindelholz, E. J.: Physical and chemical properties of sea salt deliquescent brines as a function of temperature and relative humidity, Sci. Total Environ., 824, 154462, 10.1016/j.scitotenv.2022.154462, 2022.

Castillo, A., Celeiro, M., Lores, M., Grgić, K., Banožić, M., Jerković, I., and Jokić, S.: Bioprospecting of Targeted Phenolic Compounds of Dictyota dichotoma, Gongolaria barbata, Ericaria amentacea, Sargassum hornschuchii and Ellisolandia elongata from the Adriatic Sea Extracted by Two Green Methods, Mar. Drugs, 21, 97, 10.3390/md21020097, 2023.

Cochran, R. E., Laskina, O., Jayarathne, T., Laskin, A., Laskin, J., Lin, P., Sultana, C., Lee, C., Moore, K. A., Cappa, C. D., Bertram, T. H., Prather, K. A., Grassian, V. H., and Stone, E. A.: Analysis of organic anionic surfactants in fine and coarse fractions of freshly emitted sea spray aerosol, Environ. Sci. Technol., 50, 2477-2486, 10.1021/acs.est.5b04053, 2016.

Croft, B., Martin, R. V., Moore, R. H., Ziemba, L. D., Crosbie, E. C., Liu, H., Russell, L. M., Saliba, G., Wisthaler, A., Müller, M., Schiller, A., Galí, M., Chang, R. Y. W., McDuffie, E. E., Bilsback, K. R., and Pierce, J. R.: Factors controlling marine aerosol size distributions and their climate effects over the northwest Atlantic Ocean region, Atmos. Chem. Phys., 21, 1889-1916, 10.5194/acp-21-1889-2021, 2021.

Cuadros-Orellana, S., Pohlschröder, M., and Durrant, L. R.: Isolation and characterization of halophilic archaea able to grow in aromatic compounds, Int. Biodeterior. Biodegradation, 57, 151–154, 10.1016/j.ibiod.2005.04.005, 2006.

Dekiff, J. H., Remy, D., Klasmeier, J., and Fries, E.: Occurrence and spatial distribution of microplastics in sediments from Norderney, Environ. Pollut., 186, 248–256, 10.1016/j.envpol.2013.11.019, 2014.

Deshmukh, D. K., Kawamura, K., Lazaar, M., Kunwar, B., and Boreddy, S. K. R.: Dicarboxylic acids, oxoacids, benzoic acid, α-dicarbonyls, WSOC, OC, and ions in spring aerosols from Okinawa Island in the western North Pacific Rim: size distributions and formation processes, Atmos. Chem. Phys., 16, 5263–5282, 10.5194/acp-16-5263-2016, 2016.

Di Giacinto, F., Di Renzo, L., Mascilongo, G., Notarstefano, V., Gioacchini, G., Giorgini, E., Bogdanović, T., Petričević, S., Listeš, E., Brkljača, M., Conti, F., Profico, C., Zambuchini, B., Di Francesco, G., Giansante, C., Diletti, G., Ferri, N., and Berti, M.: Detection of microplastics, polymers and additives in edible muscle of swordfish (Xiphias gladius) and bluefin tuna (Thunnus thynnus) caught in the Mediterranean Sea, J. Sea Res., 192, 102359, 10.1016/j.seares.2023.102359, 2023.

Di Renzo, L., Mascilongo, G., Berti, M., Bogdanović, T., Listeš, E., Brkljača, M., Notarstefano, V., Gioacchini, G., Giorgini, E., Olivieri, V., Silvestri, C., Matiddi, M., D'Alterio, N., Ferri, N., and Di Giacinto, F.: Potential impact of microplastics and additives on the health status of loggerhead turtles (Caretta caretta) stranded along the central adriatic coast, Water Air Soil Pollut., 232, 98, 10.1007/s11270-021-04994-8, 2021.

Ding, Z., Du, W., Wu, C., Cheng, C., Meng, J., Li, D., Ho, K., Zhang, L., and Wang, G.: Summertime atmospheric dicarboxylic acids and related SOA in the background region of Yangtze River Delta, China: Implications for heterogeneous reaction of oxalic acid with sea salts, Sci. Total Environ., 757, 143741, 10.1016/j.scitotenv.2020.143741, 2021.

Fisch, K., Waniek, J. J., and Schulz-Bull, D. E.: Occurrence of pharmaceuticals and UV-filters in riverine run-offs and waters of the German Baltic Sea, Mar. Pollut. Bull., 124, 388–399, 10.1016/j.marpolbul.2017.07.057, 2017.

Fotso Fondja Yao, C. B., Zereini, W. A., Fotso, S., Anke, H., and Laatsch, H.: Aqabamycins A–G: novel nitro maleimides from a marine Vibrio species: II. Structure elucidation*, J. Antibiot., 63, 303–308, 10.1038/ja.2010.35, 2010a.

Fotso Fondja Yao, C. B., Zereini, W. A., Fotso, S., Anke, H., and Laatsch, H.: Aqabamycins A–G: novel nitro maleimides from a marine Vibrio species: II. Structure elucidation*, The Journal of Antibiotics, 63, 303-308, 10.1038/ja.2010.35, 2010b.

Franklin, E. B., Amiri, S., Crocker, D., Morris, C., Mayer, K., Sauer, J. S., Weber, R. J., Lee, C., Malfatti, F., Cappa, C. D., Bertram, T. H., Prather, K. A., and Goldstein, A. H.: Anthropogenic and biogenic contributions to the organic composition of coastal submicron sea spray aerosol, Environ. Sci. Technol., 56, 16633–16642, 10.1021/acs.est.2c04848, 2022.

Hawas, U. W. and Abou El-Kassem, L. T.: Thalassiolin D: a new flavone O-glucoside Sulphate from the seagrass Thalassia hemprichii, Nat. Prod. Res., 31, 2369–2374, 10.1080/14786419.2017.1308367, 2017.

Hu, J., Loh, P. S., Chang, Y.-P., and Yang, C.-W.: Multi-proxy records of paleoclimatic changes in sediment core ST2 from the southern Zhejiang-Fujian muddy coastal area since 1650 yr BP, Cont Shelf Res, 239, 104717, 10.1016/j.csr.2022.104717, 2022.

Jingchuan Xue, N. S., Madhavan Elangovan, Guthrie Diamond, Kurunthachalam Kannan: Elevated accumulation of parabens and their metabolites in marine mammals from the United States coastal waters, Environ. Sci. Technol., 49, 12071–12079, 2015.

Johansson, J. H., Salter, M. E., Acosta Navarro, J. C., Leck, C., Nilsson, E. D., and Cousins, I. T.: Global transport of perfluoroalkyl acids via sea spray aerosol, Environ Sci Process Impacts, 21, 635-649, 10.1039/c8em00525g, 2019.

Kawamur, B. K. a. K.: Seasonal distributions and sources of low molecular weight dicarboxylic acids, ωoxocarboxylic acids, pyruvic acid, α-dicarbonyls and fatty acids in ambient aerosols from subtropical

Okinawa in the western Pacific Rim, Environ. Chem., 11, 673–689, 10.1071/EN14097_AC, 2014.

Klejdus, B., Plaza, M., Šnóblová, M., and Lojková, L.: Development of new efficient method for isolation of phenolics from sea algae prior to their rapid resolution liquid chromatographic–tandem mass spectrometric determination, J. Pharm. Biomed. Anal., 135, 87–96, 10.1016/j.jpba.2016.12.015, 2017.

Li, K., Guo, Y., Nizkorodov, S. A., Rudich, Y., Angelaki, M., Wang, X., An, T., Perrier, S., and George, C.: Spontaneous dark formation of OH radicals at the interface of aqueous atmospheric droplets, Proc. Natl. Acad. Sci. U.S.A., 120, e2220228120, 10.1073/pnas.2220228120, 2023.

Liao, C. and Kannan, K.: Temporal trends of parabens and their metabolites in mollusks from the Chinese Bohai Sea during 2006–2015: Species-specific accumulation and implications for human exposure, Environ. Sci. Technol., 52, 9045–9055, 10.1021/acs.est.8b02750, 2018.

Liao, C., Shi, J., Wang, X., Zhu, Q., and Kannan, K.: Occurrence and distribution of parabens and bisphenols in sediment from northern Chinese coastal areas, Environ. Pollut., 253, 759–767, 10.1016/j.envpol.2019.07.076, 2019.

Liu, L., Du, L., Xu, L., Li, J., and Tsona, N. T.: Molecular size of surfactants affects their degree of enrichment in the sea spray aerosol formation, Environ. Res., 206, 112555, 10.1016/j.envres.2021.112555, 2022a.

Liu, S., Longnecker, K., Kujawinski, E. B., Vergin, K., Bolaños, L. M., Giovannoni, S. J., Parsons, R., Opalk, K., Halewood, E., Hansell, D. A., Johnson, R., Curry, R., and Carlson, C. A.: Linkages among dissolved organic matter export, dissolved metabolites, and associated microbial community structure response in the Northwestern Sargasso Sea on a seasonal scale, Front. Microbiol., 13, 833252, 10.3389/fmicb.2022.833252, 2022b.

Lu, S., Lin, C., Lei, K., Xin, M., Wang, B., Ouyang, W., Liu, X., and He, M.: Endocrine-disrupting chemicals in a typical urbanized bay of Yellow Sea, China: Distribution, risk assessment, and identification of priority pollutants, Environ. Pollut., 287, 117588, 10.1016/j.envpol.2021.117588, 2021.

Lu, S., Wang, J., Wang, B., Xin, M., Lin, C., Gu, X., Lian, M., and Li, Y.: Comprehensive profiling of the distribution, risks and priority of pharmaceuticals and personal care products: A large-scale study from rivers to coastal seas, Water Res., 230, 119591, 10.1016/j.watres.2023.119591, 2023.

Martí-Quijal, F. J., Tornos, A., Príncep, A., Luz, C., Meca, G., Tedeschi, P., Ruiz, M.-J., and Barba, F. J.: Impact of fermentation on the recovery of antioxidant bioactive compounds from sea bass byproducts, Antioxidants, 9, 239, 10.3390/antiox9030239, 2020.

Ming, Y. and Russell, L. M.: Predicted hygroscopic growth of sea salt aerosol, J. Geophys. Res. Atmos., 106, 28259-28274, 10.1029/2001jd000454, 2001.

Mochizuki, T., Kawamura, K., Aoki, K., and Sugimoto, N.: Long-range atmospheric transport of volatile monocarboxylic acids with Asian dust over a high mountain snow site, central Japan, Atmos. Chem. Phys., 16, 14621–14633, 10.5194/acp-16-14621-2016, 2016.

mostafa, s., Mohamed, H., Ibraheem, I., and Abdel-Raouf, N.: Controlling of microbial growth by using cystoseira barbata extract, Egypt. J. Bot., 57, 469–477, 10.21608/ejbo.2017.911.1071, 2017.

Poznyakovsky, V., Kalenik, T., Wojciech, P., Tabakaeva, O., and Tabakaev, A.: Antioxidant properties of edible sea weed from the Northern Coast of the Sea of Japan, Foods Raw Mater., 9, 262–270, 10.21603/2308-4057-2021-2-262-270, 2021.

Quinn, P. K., Coffman, D. J., Johnson, J. E., Upchurch, L. M., and Bates, T. S.: Small fraction of marine cloud condensation nuclei made up of sea spray aerosol, Nat. Geosci., 10, 674–679, 10.1038/Ngeo3003, 2017.

Quinn, P. K., Collins, D. B., Grassian, V. H., Prather, K. A., and Bates, T. S.: Chemistry and related properties of freshly emitted sea spray aerosol, Chem. Rev., 115, 4383-4399, 10.1021/cr500713g, 2015.

Rastelli, E., Corinaldesi, C., Dell'Anno, A., Lo Martire, M., Greco, S., Cristina Facchini, M., Rinaldi, M., O'Dowd, C., Ceburnis, D., and Danovaro, R.: Transfer of labile organic matter and microbes from the ocean surface to the marine aerosol: an experimental approach, Sci. Rep., 7, 11475, 10.1038/s41598-017-10563-z, 2017.

Ren, L., Weng, L., Chen, D., Hu, H., Jia, Y., and Zhou, J. L.: Bioremediation of PAEs-contaminated saline soil: The application of a marine bacterial strain isolated from mangrove sediment, Mar. Pollut. Bull., 192, 115071, 10.1016/j.marpolbul.2023.115071, 2023a.

Ren, L., Weng, L., Chen, D., Hu, H., Jia, Y., and Zhou, J. L.: Bioremediation of PAEs-contaminated saline soil: The application of a marine bacterial strain isolated from mangrove sediment, Marine Pollution Bulletin, 192, 115071, 10.1016/j.marpolbul.2023.115071, 2023b.

Rosenfeld, D., Zhu, Y., Wang, M., Zheng, Y., Goren, T., and Yu, S.: Aerosol-driven droplet concentrations dominate coverage and water of oceanic low-level clouds, Science, 363, 599–614, 10.1126/science.aav0566, 2019.

Rukachaisirikul, V., Khamthong, N., Sukpondma, Y., Phongpaichit, S., Hutadilok-Towatana, N., Graidist, P., Sakayaroj, J., and Kirtikara, K.: Cyclohexene, diketopiperazine, lactone and phenol derivatives from the sea fan-derived fungi Nigrospora sp. PSU-F11 and PSU-F12, Arch. Pharm. Res., 33, 375–380, 10.1007/s12272-010-0305-3, 2010.

Salter, M. E., Nilsson, E. D., Butcher, A., and Bilde, M.: On the seawater temperature dependence of the sea spray aerosol generated by a continuous plunging jet, J. Geophys. Res. Atmos., 119, 9052-9072, 10.1002/2013jd021376, 2014.

Sanjuan, O. N., Sait, S. T. L., Gonzalez, S. V., Tomás, J., Raga, J. A., and Asimakopoulos, A. G.: Phthalate metabolites in loggerhead marine turtles (Caretta caretta) from the Mediterranean Sea (East Spain region), Environ. Toxicol. Chem., 5, 178–185, 10.1016/j.enceco.2023.08.003, 2023.

Sha, B., Johansson, J. H., Benskin, J. P., Cousins, I. T., and Salter, M. E.: Influence of water concentrations of perfluoroalkyl acids (PFAAs) on their size-resolved enrichment in nascent sea spray aerosols, Environ. Sci. Technol., 55, 9489–9497, 10.1021/acs.est.0c03804, 2021.

Shao, C., Guo, Z., Peng, H., Peng, G., Huang, Z., She, Z., Lin, Y., and Zhou, S.: A new isoprenyl phenyl ether compound from mangrove fungus, Chem Nat Compd, 43, 377–380, 10.1007/s10600-007-0142-x, 2007.

Shumilina, E., Skavang, P. K., and Dikiy, A.: Application of NMR spectroscopy for the detection and quantification of phthalic acid in fish muscles: The case of Atlantic Cod from Norwegian Sea, Mar. Environ. Res., 188, 105973, 10.1016/j.marenvres.2023.105973, 2023.

Simoneit, B. R. T.: Biomass burning- a review of organic tracers for smoke from incomplete combustion, Appl. Geochem., 17, 129–162, 10.1016/S0883-2927(01)00061-0, 2022.

Tang, I. N., Tridico, A. C., and Fung, K. H.: Thermodynamic and optical properties of sea salt aerosols, J. Geophys. Res. Atmos., 102, 23269-23275, 10.1029/97jd01806, 1997.

Tian, M., Zhu, T., Park, H. E., and Row, K. H.: Purification of 4-hydroxybenzoic acid and 4-hydroxybenzaldehyde from Laminaria japonica aresch using commercial and monolithic sorbent in SPE cartridge, Anal. Lett., 45, 2359–2366, 10.1080/00032719.2012.691590, 2012.

Wang, J., Yao, P., Bianchi, T. S., Li, D., Zhao, B., Cui, X., Pan, H., Zhang, T., and Yu, Z.: The effect of particle density on the sources, distribution, and degradation of sedimentary organic carbon in the Changjiang Estuary and adjacent shelf, Chem. Geol., 402, 52–67, 10.1016/j.chemgeo.2015.02.040, 2015.

Wilson, T. W., Ladino, L. A., Alpert, P. A., Breckels, M. N., Brooks, I. M., Browse, J., Burrows, S. M., Carslaw, K. S., Huffman, J. A., Judd, C., Kilthau, W. P., Mason, R. H., McFiggans, G., Miller, L. A., Najera, J. J., Polishchuk, E., Rae, S., Schiller, C. L., Si, M., Temprado, J. V., Whale, T. F., Wong, J. P., Wurl, O., Yakobi-Hancock, J. D., Abbatt, J. P., Aller, J. Y., Bertram, A. K., Knopf, D. A., and Murray, B. J.: A marine biogenic source of atmospheric ice-nucleating particles, Nature, 525, 234-238, 10.1038/nature14986, 2015.

Xu, F., Jin, H., Ji, Z., Chen, J., and Loh, P. S.: Sources and distribution of sedimentary organic matter along the northern Bering and Chukchi Seas, J Environ Sci (China), 52, 66–75, 10.1016/j.jes.2016.04.003, 2017.

Xu, W., Ovadnevaite, J., Fossum, K. N., Lin, C. S., Huang, R. J., Ceburnis, D., and O'Dowd, C.: Sea spray as an obscured source for marine cloud nuclei, Nat. Geosci., 15, 282–286, 10.1038/s41561-022-00917-2, 2022.

Xuefeng Zhou, X. L., Xieyang Guo, Bin Yang, Xian-Wen Yang and Yonghong Liu: Chemical constituents of the sponge mycale species from South China Sea, Rec. Nat. Prod., 7, 119–123, 2013.

Yang, J., Zhao, W., Wei, L., Zhang, Q., Zhao, Y., Hu, W., Wu, L., Li, X., Pavuluri, C. M., Pan, X., Sun, Y., Wang, Z., Liu, C.-Q., Kawamura, K., and Fu, P.: Molecular and spatial distributions of dicarboxylic acids, oxocarboxylic acids, and α-dicarbonyls in marine aerosols from the South China Sea to the eastern Indian Ocean, Atmos. Chem. Phys., 20, 6841–6860, 10.5194/acp-20-6841-2020, 2020.

Zangrando, R., Corami, F., Barbaro, E., Grosso, A., Barbante, C., Turetta, C., Capodaglio, G., and Gambaro, A.: Free phenolic compounds in waters of the Ross Sea, Sci. Total Environ., 650, 2117–2128, 10.1016/j.scitotenv.2018.09.360, 2019.

Zhao, X., Qiu, W., Zheng, Y., Xiong, J., Gao, C., and Hu, S.: Occurrence, distribution, bioaccumulation, and ecological risk of bisphenol analogues, parabens and their metabolites in the Pearl River Estuary, South China, Ecotoxicol. Environ. Saf., 180, 43–52, 10.1016/j.ecoenv.2019.04.083, 2019.

Zhu, Y., Tilgner, A., Hans Hoffmann, E., Herrmann, H., Kawamura, K., Xue, L., Yang, L., and Wang, W.: Molecular distributions of dicarboxylic acids, oxocarboxylic acids, and α-dicarbonyls in aerosols over Tuoji Island in the Bohai Sea: Effects of East Asian continental outflow, Atmos Res, 272, 106154, 10.1016/j.atmosres.2022.106154, 2022.